Vol 18 No 8, August 2009
1674-1056/2009/18(08)/3555-08

Chinese Physics B

© 2009 Chin. Phys. Soc.
and IOP Publishing Ltd

Structure and luminescence of $Ca_2Si_5N_8$:Eu^{2+} phosphor for warm white light-emitting diodes*

Wei Xiao-Dan(魏小丹)[a], Cai Li-Yan(蔡丽艳)[a], Lu Fa-Chun(鲁法春)[a],
Chen Xiao-Long(陈小龙)[b], Chen Xue-Yuan(陈学元)[c], and Liu Quan-Lin(刘泉林)[a]†

[a] *School of Materials Science & Engineering and State Key Laboratory for Advanced Metals and Materials, University of Science and Technology Beijing, Beijing* 100083, *China*
[b] *Beijing National Laboratory for Condensed Matter Physics, Institute of Physics, Chinese Academy of Sciences, Beijing* 100190, *China*
[c] *Fujian Institute of Research on the Structure of Matter, Chinese Academy of Sciences, Fuzhou* 350002, *China*

(Received 24 October 2008; revised manuscript received 19 January 2009)

We have synthesized $Ca_2Si_5N_8$:Eu^{2+} phosphor through a solid-state reaction and investigated its structural and luminescent properties. Our Rietveld refinement of the crystal structure of $Ca_{1.9}Eu_{0.1}Si_5N_8$ reveals that Eu atoms substituting for Ca atoms occupy two crystallographic positions. Between 10 K and 300 K, $Ca_2Si_5N_8$:Eu^{2+} phosphor shows a broad red emission band centred at ∼1.97 eV–2.01 eV. The gravity centre of the excitation band is located at 3.0 eV–3.31 eV. The centroid shift of the 5*d* levels of Eu^{2+} is determined to be ∼1.17 eV, and the red-shift of the lowest absorption band to be ∼ 0.54 eV due to the crystal field splitting. We have analysed the temperature dependence of PL by using a configuration coordinate model. The Huang–Rhys parameter $S = 6.0$, the phonon energy $\hbar\nu = 52$ meV, and the Stokes shift $\Delta S = 0.57$ eV are obtained. The emission intensity maximum occurring at ∼200 K can be explained by a trapping effect. Both photoluminescence (PL) emission intensity and decay time decrease with temperature increasing beyond 200 K due to the non-radiative process.

Keywords: luminescence, structure，nitride, europium, white light-emitting diode (LED)
PACC: 7855H, 8120N, 6160

1. Introduction

White light-emitting diode (LED) has increasingly attracted attention as a new light source because of its energy-saving, long lifetime, low operating voltage, compactness and friendly environment.[1] The white light can be generated by using an LED chip-phosphor system, in which the phosphor strongly absorbs ultraviolet (UV)-blue light (370–460 nm) from the LED chip and efficiently re-emits in the red, or green, or yellow blue part of the visible spectrum. The first commercially available white LED, which featured a combination of a blue LED with a yellow $(Y_{1-a}Gd_a)_3(Al_{1-b}Ga_b)O_{12}$:$Ce^{3+}$ (YAG:Ce) phosphor, was realized in 1996.[2] However, this type of white light has poor colour rendering because it lacks a red component. Restricted by very low absorption in the emission range of the blue LED chip, the well-developed phosphors used for current mercury gas-discharge fluorescent lamps cannot be directly applied to white LED lighting. To develop warm-white LEDs with a higher colour rendering index, many investigations have been carried out to search for novel red-emitting phosphors, which can be excited by blue (∼460 nm) or UV (∼400 nm) LEDs.

The emission and the absorption spectra of the Eu^{2+} ion usually consist of broad bands due to transitions between the $^8S_{7/2}$ ground level of the $4f^7$ configuration and the crystal field components of the $4f^6 5d$ excited state. The emission varies from UV to red, depending on the host lattice. In many halide or oxide hosts, luminescence of Eu^{2+} is found in a wavelength region of near UV to blue.[3] Meanwhile, in oxynitrides such as α-SiAlON,[4] Eu^{2+} emits light in green or yellow; and in some nitrides or sulfides it emits light in a green-to-red region.[5,6] This trend reflects the well-known nephelauxetic effect, which was attributed to the increase of covalency between the lanthanide ion and the anion ligands a long time ago.[7] Dorenbos

*Project supported by the National Natural Science Foundation of China (Grant No 50672007), Program for the New Century Excellent Talents of China (Grant No NCET-06-0082), and the National Basic Research Program of China (Grant No 2007CB936202).
†Corresponding author. E-mail: qlliu@mater.ustb.edu.cn

has carried out a systematic study of the energy of the first $4f^7 \rightarrow 4f^6 5d$ transition of Eu^{2+} in inorganic compounds.[8] However, the sulfide-based phosphors have poor chemical stabilities, thereby causing the strong temperature dependence of chromaticity and degradation of the luminous efficiency of the white LEDs. Currently, there is increasing interest in nitridosilicates $M_2Si_5N_8$:Eu^{2+} (M=Ca, Sr, Ba) due to their potential application in warm white LEDs.[9,10]

Several synthetic strategies for $M_2Si_5N_8$:Eu^{2+} have been reported in the literature. The first one involves the reaction of a stoichiometric amount of barium metal (Ba) and europium metal (Eu) with silicon diimide ($Si(NH)_2$) at 1650 °C in a radio frequency furnace.[11] The second one involves the reaction of strontium nitride (Sr_3N_2) and europium nitride (EuN) with silicon nitride (Si_3N_4).[10] The above two synthetic processes were handled in a dry glovebox flushed with dry nitrogen because of air and water sensitivity of some of the starting materials. Piao *et al* [12] reported on the carbothermal reduction and nitridation method to synthesize $Sr_2Si_5N_8$:Eu^{2+} phosphor. In this method, residual carbon is incorporated into phosphor, thereby reducing its intensities of absorption and emission. Xie *et al* [13] reported that $Sr_2Si_5N_8$:Eu^{2+}-based phosphors could be prepared through a solid-state reaction between $SrCO_3$,Eu_2O_3 and Si_3N_4. This method is free from carbon, but it requires high temperature (1873 K) and high N_2-gas-pressure (∼5 nitrogen atmosphere).

Here, we report on a novel synthetic route to $Ca_2Si_5N_8$:Eu based on a direct reaction among $CaSi_2$, Eu_2O_3 and Si_3N_4 at 1873 K and in a nitrogen atmosphere. All the raw materials are commercially available, and the handling and mixing of raw powders can be done in an ambient atmosphere. The crystal structure of $Ca_2Si_5N_8$:Eu is analysed by the Rietveld refinement of the x-ray diffraction (XRD) data. We investigate the properties of the main characteristics of Eu^{2+} emission and absorption at low temperatures, including the crystal field splitting, the red shift, the influence of the lattice vibration (electron-phonon coupling), the temperature dependence of emission, and the thermal quenching of the luminescence.

2. Experiments

The $(Ca_{1-x}Eu_x)_2Si_5N_8$ (x = 0, 0.02, 0.05, 0.1, 0.2) powder samples were prepared by a solid-state reaction. The starting materials were high-purity $CaSi_2$ (99.9%), Si_3N_4 (99.99%), and Eu_2O_3 (99.99%). The raw powders were weighted according to the stoichiometric compositions, and then mixed, ground and pressed into pellets sequentially. The pellets were sintered at 1873 K for 2 h in a graphite furnace under a nitrogen atmosphere.

X-ray powder diffraction (XRD) data used for structure analysis were collected on a Rigaku D/max 2500 diffractometer with Cu Kα radiation (50 kV×250 mA) and a graphite monochromator. A step scan mode was employed in steps of $2\theta = 0.02°$ and with a sampling time of 1 s. The XRD data were analysed by the Rietveld refinement program FullProf.2k (Version 2.40) based on the structure model of $Ca_2Si_5N_8$ reported by Schlieper *et al*.[14] The Pseudo–Viogt function was used as a profile function.

Emission and excitation spectra and transient decays were recorded on an Edinburgh Instruments FLS920 spectrofluorimeter equipped with both continuous (450 W) xenon and pulsed xenon or hydrogen lamps. For low-temperature measurements, samples were mounted on a closed cycle cryostat (10–350 K, DE202, Advanced Research Systems).

3. Results and analysis

The detailed analysis of the XRD patterns of samples $(Ca_{1-x}Eu_x)_2Si_5N_8$ (x = 0, 0.02, 0.05, 0.1, 0.2) shows that their phase compositions depend on the concentration of Eu. When $0 \leq x < 0.1$, the sample is of almost $(Ca_{1-x}Eu_x)_2Si_5N_8$ single phase with a very small amount of α-Si_3N_4 as impurity. A further increase of Eu concentration leads to the formation of Si_3N_4 and $EuSiO_3$, both as impurities. These observations indicate that the solubility of Eu^{2+} in $Ca_2Si_5N_8$ is very limited, probably, to a range of 0–0.1, i.e. $0 \leq x < 0.1$, compared well with the result reported by Li *et al*.[5] Such a limitation may be due to two causes. One is the difference in crystal structure: $Ca_2Si_5N_8$ is monoclinic while $Eu_2Si_5N_8$ is orthorhombic. The other is the difference in ionic radius: the radius of Eu^{2+}(1.17 Å) (1 Å=0.1 nm) is obviously larger than that of Ca^{2+}(1.00 Å) (the radius data are taken from the periodic table of elements). In Table 1 the lattice parameters of $Ca_2Si_5N_8$ and $Ca_{1.9}Eu_{0.1}Si_5N_8$ compounds are listed and compared with those of the previous reports.[10,12,14] It is observed from our work that $\boldsymbol{a}$, $\boldsymbol{b}$, and c, V of $Ca_{1.9}Eu_{0.1}Si_5N_8$ are increased

with respect to those of $Ca_2Si_5N_8$, which is in accordance with Vegard's law. This is a strong indication that Eu^{2+} ions have been substituted for Ca^{2+}ions in the lattice. The oxygen impurity from a very small amount of Eu_2O_3 content is effectively removed by sintering $(Ca_{1-x}Eu_x)_2Si_5N_8$ at 1873 K under a nitrogen atmosphere in a graphite furnace.

Table 1. Lattice parameters of $(Ca_{1-x}Eu_x)_2Si_5N_8$ compounds.

	a/Å	b/Å	c/Å	β/(°)	V/Å^3	Ref.
$Ca_2Si_5N_8$	14.3387(4)	5.6114(2)	9.6925(3)	112.11(2)	722.5	this work
$Ca_2Si_5N_8$	14.352	5.610	9.689	112.06	723.0	14
$Ca_2Si_5N_8$	14.3404	5.6138	9.6782	112.13	721.7	12
$Ca_{1.9}Eu_{0.1}Si_5N_8$	14.3430(4)	5.6143(2)	9.6952(3)	112.13(2)	723.2	this work
$Ca_{1.9}Eu_{0.1}Si_5N_8$	14.3377	5.6087	9.6835	112.09	721.5	10

The Rietveld powder diffraction profile fitting technique[15] is adopted to refine the crystal structure of $Ca_{1.9}Eu_{0.1}Si_5N_8$ through using the program FullProf.2k. The initial structure model was built based on the structure of $Ca_2Si_5N_8$ reported by Schlieper and Schnick.[14] Due to the large difference in atomic scattering factor between Ca and Eu, the preferential occupation of Eu on different crystallographic positions can be determined successfully by the Rietveld refinement. During the refinement, we locate Eu atoms on two Ca-occupied sites, and then refine the occupancies on the two sites as free parameters. According to the refinement results of Eu occupancy, the chemical composition of the compound is $Ca_{1.91}Eu_{0.09}Si_5N_8$, which is identical with the nominal composition, $Ca_{1.9}Eu_{0.1}Si_5N_8$, within the experimental error. This suggests that the refinement results of the crystallographic position and occupancy of Eu are reliable. The next investigations regarding luminescent properties are focused on the sample $Ca_{1.9}Eu_{0.1}Si_5N_8$.

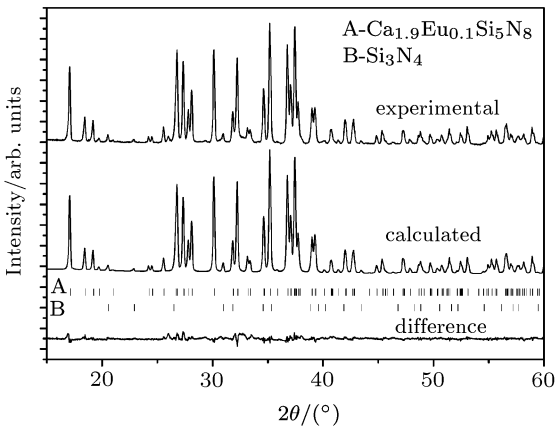


Fig.1. Rietveld refinement results of the XRD patterns of the $Ca_{1.9}Eu_{0.1}Si_5N_8$ compound, including the experimental and calculated intensities as well as differences in intensity between experimental and calculated data. The middle vertical bars indicate Bragg reflection positions of $Ca_{1.9}Eu_{0.1}Si_5N_8$ (A) and α-Si_3N_4 (B).

Figure 1 shows the Rietveld refinement results of the XRD patterns of the sample $Ca_{1.9}Eu_{0.1}Si_5N_8$, including the experimental and calculated data. The pattern factor R_p, the weighted pattern factor R_{wp}, and the expected pattern factor R_{exp}, are 10.1, 13.0 and 5.25%, respectively. The structural parameters, including lattice parameters, atomic positions and occupancy, are listed in Table 2.

Table 2. Rietveld refinement results for the $Ca_{1.9}Eu_{0.1}Si_5N_8$ compound; space group C_c; lattice parameter; atomic position and occupancy; pattern factor R_p; weighted pattern factor R_{wp}; expected pattern factor R_{exp}.

atoms	site	X	Y	Z	Occ
Ca1	4a	0.0000	0.7734	0.0000	0.951
Eu1	4a	0.0000	0.7734	0.0000	0.049
Ca2	4a	0.6126	0.7543	0.2044	0.960
Eu2	4a	0.6126	0.7543	0.2044	0.040
Si1	4a	0.0617	0.8045	0.3577	1.000
Si2	4a	0.7555	0.2067	0.3204	1.000
Si3	4a	0.7571	0.4866	0.0630	1.000
Si4	4a	0.3606	0.2111	0.3656	1.000
Si5	4a	0.8572	-0.0040	0.1275	1.000
N1	4a	0.9872	0.6405	0.4169	1.000
N2	4a	0.1318	0.0173	0.9909	1.000
N3	4a	0.7967	0.2587	0.1677	1.000
N4	4a	0.8059	0.7526	0.1762	1.000
N5	4a	0.9833	0.0199	0.2138	1.000
N6	4a	0.8313	-0.0036	0.9381	1.000
N7	4a	0.6312	0.1538	0.2643	1.000
N8	4a	0.7991	0.4940	0.4205	1.000

Space group C_c, a=14.3431(1), b=5.6144(1),
c=9.6953(1)(Å), β=112.13(1)(°)
R_p = 10.1%, R_{wp} = 13.0%, R_{exp} = 5.25%

There exists a small amount of α-Si_3N_4 as impurities in the samples. The weight fraction of the α-Si_3N_4 phase and the $Ca_{1.9}Eu_{0.1}Si_5N_8$ phase can be calculated via the following relation based on Rietveld refinement results:[16]

$$W_1 = \frac{S_1 Z_1 M_1 V_1}{S_1 Z_1 M_1 V + S_2 Z_2 M_2 V_2},$$

where S_i is the refined scale factor, $Z_i M_i$ is the weight of the unit cell in atomic weight units, and V_i is the volume of the unit cell. The mass fraction of α-Si_3N_4 in sample $Ca_{1.9}Eu_{0.1}Si_5N_8$ is calculated to be about 4.4%.

The PL emission spectra of $Ca_{1.9}Eu_{0.1}Si_5N_8$ between 10 K and 300 K in intervals of 50 K, excited by a xenon lamp operating at 372 nm, are shown in Fig.2. The PL spectra are recorded under the same conditions except for temperature; therefore, the relative intensities are directly comparable. The PL spectra are shifted upward by a certain intensity value to improve their visual observation. All spectra present a broad band, which is attributed to the electric dipole-allowed transition from the $4f^6(^7F)5d$ excited state to the $4f^7$ ($^8S_{7/2}$) ground state of the Eu^{2+} ions. The narrow emission lines from the Eu^{3+} intra-$4f^n$ shell

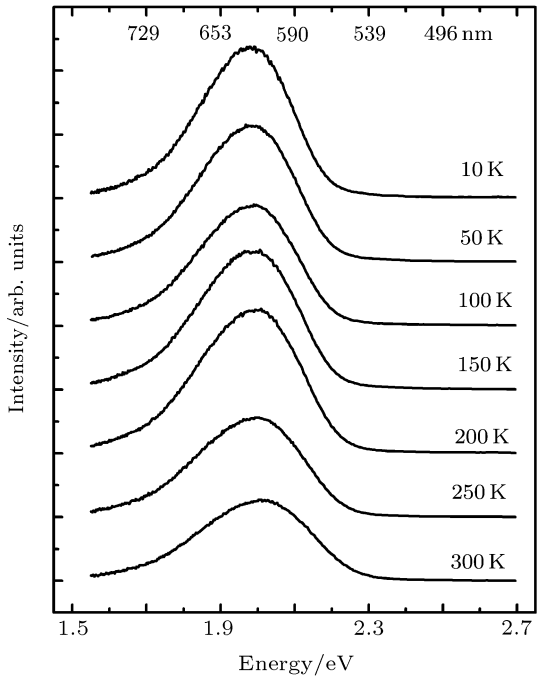


Fig.2. PL emission spectra of $Ca_{1.9}Eu_{0.1}Si_5N_8$ between 10 K and 300 K in intervals of 50 K, excited by a xenon lamp operating at 372 nm. Spectra are offset vertically to improve visual observation.

transitions ($^5D_0 \rightarrow {}^7F_J$) are not observed. These results indicate that Eu atoms behave as Eu^{2+} ions in the host structure. The centres of gravity of the emission ε_{em} are listed in Table 3. The ε_{em} shifts toward short wavelengths from 1.97 eV to 2.01 eV with the increase of temperature, which can be ascribed to the increase of the energy for the occupied vibration level of the emitting electronic state.

Table 3. Luminescence data of $Ca_{1.9}Eu_{0.1}Si_5N_8$ compound at different temperatures, including centre of gravity (ε_{em}) of the emission band, full width at half maximum ($FWHM_{em}$) of the emission band, centre of gravity (ε_{ex}) of the excitation band, and decay time (τ).

temperature/K	ε_{em}/eV	$FWHM_{em}$/meV	ε_{ex}/eV	decay/μs
10	1.97	293	3.05	0.98
50	1.97	303	3.05	0.93
100	1.99	309	3.00	0.93
150	2.01	313	3.31	0.90
200	2.01	326	3.31	0.91
250	2.00	330	3.05	0.83
300	2.01	350	3.05	0.76

The spectrum at 300 K is plotted again in Fig.3, in order to better display the shape of the emission band. The broad emission band is not symmetric, which can be fitted into two Gaussians centred at ~1.90 eV and ~2.04 eV. They may be caused by two crystallographic Eu^{2+} sites (see Table 2). In the structure of the $Ca_{1.9}Eu_{0.1}Si_5N_8$ compound, Eu atoms occupy two crystallographic positions. Each Eu site is coordinated with seven N atoms. The distances of Ca1 (Eu1) to the neighbouring N are 0.244 (N1), 0.236 (N2), 0.258 (N5a), 0.293 (N5b), 0.259 (N6), 0.263 (N7) and 0.309 (N8) nm, respectively. The distances of Ca2 (Eu2) to the neighbouring N are 0.276 (N1), 0.256 (N2a), 0.309 (N2b), 0.289 (N4), 0.230 (N5), 0.231 (N7), and 0.308 (N8) nm, respectively. The mean distance of Eu1-N is smaller than that of Eu2-N [Eu1-N=0.266 nm and Eu2-N=0.271 nm]. The Eu^{2+} ions at the Eu1 sites experience a stronger crystal-field, which is inversely proportional to R^5 (R is the chemical bond length between a cation and the coordinating anion),[17] resulting in a longer emission wavelength. Therefore, the two emission bands centred at ~1.90 eV and ~2.04 eV can be attributed to Eu^{2+} ions at Eu1 and Eu2 crystallographic sites, respectively.

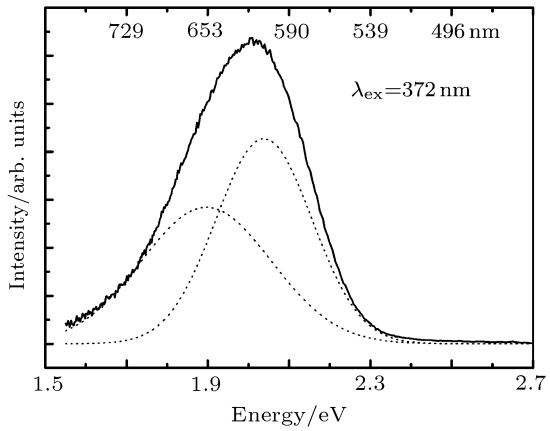


Fig.3. The PL emission spectrum at 300 K (solid lines), illustrating curve-fitting results by two Gaussians (dashed lines).

The temperature dependence of the total integrated PL intensity of Eu^{2+} emission bands, calculated from Fig.2, is plotted in Fig.4. The integrated PL intensity first decreases with temperature increasing, then increases in a range of 100–200 K. Above 200 K, the emission intensity again decreases with temperature increasing. The quenching temperature is evaluated to be ∼360 K by linearly extrapolating the intensity to half the maximum intensity in Fig.4. This variation is different from the previous result,[10] where the emission intensity of $Ca_{1.9}Eu_{0.1}Si_5N_8$ monotonously decreases with temperature increasing. The appearing of emission intensity maximum in our work can be explained by the trapping effect.[18] The trap states are related to defects or nitrogen vacancies formed during the synthesis.[11] Initially the electrons (or holes) are excited and afterwards trapped by defects. The trapped electrons (or holes) are then thermally released to the excited Eu^{2+}-states, resulting in emission intensity that is enhanced with the increase of temperature.

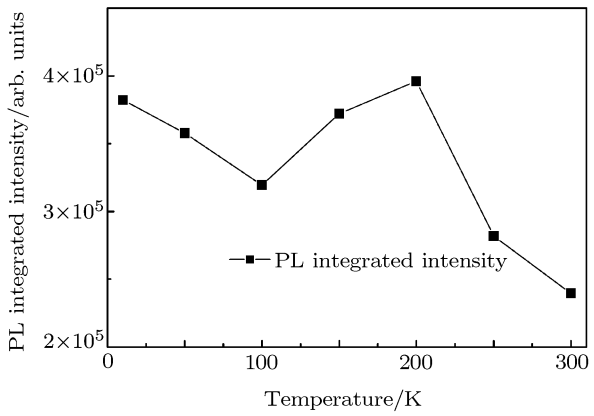


Fig.4. Total integrated PL intensity of $Ca_{1.9}Eu_{0.1}Si_5N_8$ as a function of temperature.

On the other hand, the thermal quenching effect of PL becomes strong as temperature increases, leading the emission intensity to decrease. The subtle combination of the above two processes can give rise to a complex temperature dependence of the emission intensity, causing a maximum to appear at about 200 K.

The full widths at half maximum (FWHMs) of the emission bands are each plotted as a function of temperature in Fig.5 (the data are listed in Table 3). The FWHMs rise from 303 meV at 50K to 350 meV at 300 K with temperature increasing. The temperature dependence of the FWHM can be described by using the configurational coordinate model according to the following formula:[19]

$$\mathrm{FWHM} = 2.36 \times h\nu \times \sqrt{S} \times \sqrt{\coth\left(\frac{h\nu}{2kT}\right)},$$

where $h\nu$ is the phonon energy, k the Boltzmann constant, T the Kelvin temperature and S the Huang-Rhys parameter. The Huang–Rhys parameter S is the electron-phonon coupling strength, a dimensionless number that represents the average number of phonons created during lattice relaxation subsequent to the electronic transition. This formula can be applied only to the situation where there are the same curvatures for both ground and excited parabolas in a configuration coordination diagram. The best fitting of the above formula to the observed data, with $S = 6.0$ (5) and $h\nu = 52$ (3) meV, is shown as a solid line in Fig.5.

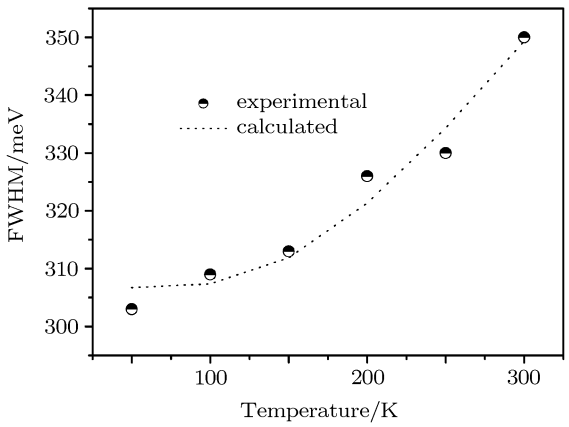


Fig.5. Full widths at half maximum (FWHMs) of the emission band vs temperature.

Figure 6 shows the excitation spectra of $Ca_{1.9}Eu_{0.1}Si_5N_8$ with a monitor wavelength 612 nm, measured at different temperatures. The excitation spectra are recorded under the same conditions except for temperature; therefore, the relative intensities are

directly comparable. The PL spectra are shifted upwards by a certain intensity value to improve their visual observation. All spectra present almost the same features. The gravity centres of the excitation band at different temperatures are listed in Table 3. Several sub-bands can be distinguished at 300 K, centred at about 2.51, 3.00, 3.32, 4.30 eV, separately. If one of the $4f$ electrons of Eu^{2+} is promoted to the $5d$ level, it leaves six electrons in the lower $4f$ configuration. This is a ^7F_J term the same as that in the case of Eu^{3+} ($4f^6$). This term always gives the total-symmetric representation of the site-symmetry group involved. The promoted electron occupies the $5d$ level, which is split by the crystal field. In the host lattice of the $Ca_{1.9}Eu_{0.1}Si_5N_8$ compound, the symmetry of the Eu^{2+} site is extremely low, i.e. the site symmetry is 1. The number of Eu^{2+}-absorption bands is therefore up to a maximum of five. Based on the lowest and highest excitation bands, the crystal-field splitting $\varepsilon_{\rm cfs}$ is calculated to be about 1.79 eV.

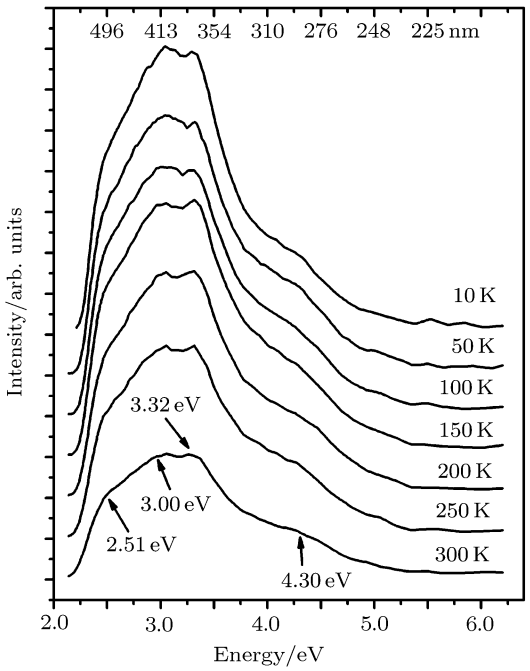


Fig.6. Excitation spectra of $Ca_{1.9}Eu_{0.1}Si_5N_8$ at different temperatures, monitored at 612 nm. Spectra are offset vertically to improve visual observation.

Figure 7 shows a comparison between the excitation and the emission spectra of the $Ca_{1.9}Eu_{0.1}Si_5N_8$ compound measured at 300 K. It is found that the emission and the excitation band shapes are almost mirror images of each other. This relationship strongly suggests that in a configuration coordinate diagram the energies of phonons are all equal to $h\nu$ both for the ground states $4f^7(^8S_{7/2})$ and for the excited states $4f^65d^1$, and both the states have parabolas with the same curvatures. The energy of the zero-phonon line E_0 at the intersection of the emission and the excitation bands is measured to be 2.23 eV. The zero-line corresponds to a transition between purely electronic states.

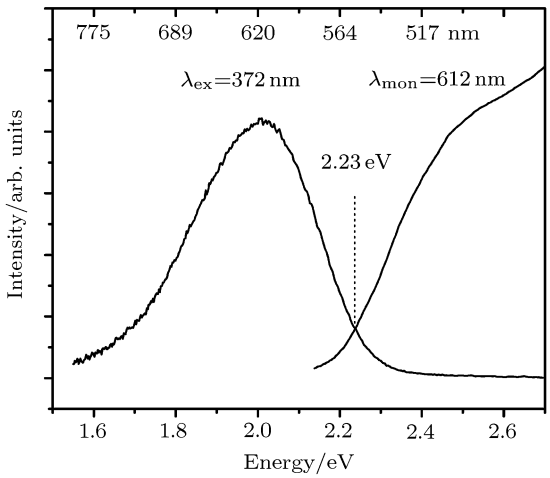


Fig.7. Comparison between the excitation spectrum and the emission spectrum at 300 K, illustrating the almost mirror-image relation.

Luminescence decay curves of $Ca_{1.9}Eu_{0.1}Si_5N_8$ are measured at various temperatures. The curves can be well characterized by single exponential decays. The fitted profile of the luminescence decay can be expressed as the following expression $I(t) = A_0 + A_1 \exp\{-t/\tau\}$, where $I(t)$ is the photoluminescence intensity, A_0 and A_1 are the constants, and τ is the decay time for the exponential component. The decay times at different temperatures are obtained and listed in Table 3 (the goodness of fitting $R > 99.5\%$). As an example, the experimental decay data and the fitted decay curve at 50 K are shown in Fig.8. The $5d \rightarrow 4f$ transition is an allowed electric dipole transition and therefore the decay time of the fluorescence is very short ($< 10^{-6}$ sec). The decay time between 50 K and 200 K remains almost the same. Beyond 200 K, a strong decrease of decay time occurs with temperature increasing. Above 200 K, both integrated PL intensities and decay times decrease with temperature increasing; these phenomena can be ascribed to the non-radiative process dominating.

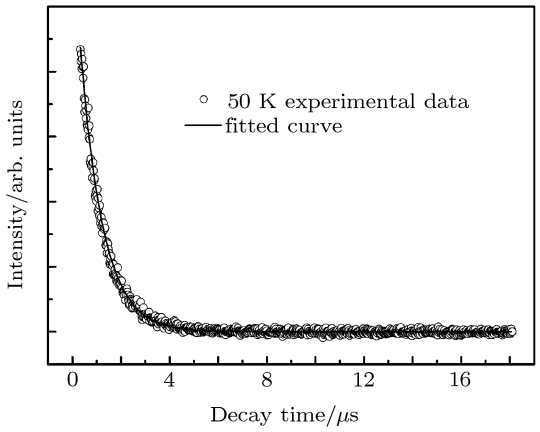


Fig.8. Luminescence decay curve of $Ca_{1.9}Eu_{0.1}Si_5N_8$ at 50 K, monitoring at 621 nm under excitation at 372 nm, and fitted curve.

4. Discussion

The luminescent properties of RE ions usually involve two electric transitions: intra-$4f^n$ ($4f$–$4f$) transition and $4f^n$–$4f^{n-1}5d$ transition (transition between a $4f^{n-1}5d^1$ excited state and a $4f^n$ ground state). The emission wavelength from the intra-$4f^n$ transition of trivalent RE ions is relatively insensitive to the host and the temperature because the $4f$ shell is shielded from its surroundings by the filled $5s$ and $5p$ shells. The $4f^n$–$4f^{n-1}5d^1$ transition is an allowed electric dipole transition and therefore broad emissions can be achieved. In addition, the wavelengths of absorption and emission can be tuned by the host lattice because of the strong interaction of the $5d$-electron with the neighbouring anion ligands in the compounds. Dorenbos[8] has carried out a systematic study of the energies of the lowest $4f^{n-1}5d^1$ states of Eu^{2+} ions. The effect of the host crystal on the energy difference of fd-absorption is expressed as the energy red-shift of $5d$ levels. This red-shift is a combined effect of the centroid shift ε_c and the crystal field splitting ε_{cfs}. The centroid shift ε_c is the downward shift of the average energy of the five $5d$ levels of Eu^{2+} relative to the energy of the first fd transition in the free Eu^{2+} ion. ε_c represents the nephelauxetic effect which is often attributed to covalency between the lanthanide ion and the anion ligands of the host lattice.[20] The crystal-field splitting ε_{cfs} is the difference in energy between the lowest and highest $5d$ levels.

In the present work, the centre of gravity (ε_{ex}) of the excitation bands of $Ca_{1.9}Eu_{0.1}Si_5N_8$ is measured to be about 3.05 eV at 300 K. We can calculate the centroid shift ε_c from the difference between the centre of gravity (ε_{ex}) of the excitation bands and the energy of the first fd transition in the free Eu^{2+} ion (~ 4.22 eV),[8] i.e. $\varepsilon_c = 1.17$ eV (4.22–3.05=1.17 eV). The lowest absorption band at 300 K is observed to be 2.51 eV as shown in Fig.6. The red-shift of the lowest absorption band (i.e. 3.05–2.51=0.54 eV) is due to the crystal field splitting. Compared with the excitation band of Eu^{2+}-doped halides and oxides, there is a large redshift of $5d$ levels. This phenomenon can be explained as follows: A large centroid shift ε_c arises from an increase in covalency (nephelauxetic effect) when Eu^{2+} coordinates to the less electronegative nitrogen than oxygen or halogen. The crystal field splitting ε_{cfs} of the $5d$ band increases when the higher formal charge of N^{3-} coordinates to the Eu^{2+} ion versus O^{2-} or Cl^{1-}.

The emission bands are further lowered by Stokes shift ΔS. The Stokes shift (ΔS) has a magnitude of $(2S-1)\,h\nu$ that is related to the offset of the parabolas in the configuration coordination diagram. Based on the above values of $S = 6.0$ and $\hbar\nu = 52$ meV, the stokes shift ΔS is calculated to be 0.57 eV. According to the mirror-image relationship between the emission and the excitation spectra, and the energy of the zero-phonon line ($E_0 = 2.23$ eV, see Fig.7), we can calculate the energy E_{fd} of fd transition from the ground state to the lowest level of the $4f^6 5d$ excited state from $E_{fd} = E_0 + \Delta S/2$ to be 2.51 eV, i.e. $E_{fd} = 2.51$ eV. This value accords with the value where the observed excitation peak appears, 2.51 eV, in Fig.6. We can also evaluate the energy E_{df} of the df transition from the lowest level of the $4f^6 5d$ excited state to the ground state from $E_{df} = E_0 - \Delta S/2$ to be 1.95 eV, i.e. $E_{df} = 1.95$ eV. This value is almost consistent with the value where the observed emission peak occurs, 2.01 eV, in Fig.2.

$Ca_{1.9}Eu_{0.1}Si_5N_8$ phosphor has a much larger Stokes shift, 0.57 eV. Generally speaking, a large displacement between ground and excited states in a configuration coordinate diagram (giving a large Stokes shift) will involve a high probability of non-radiative transitions (i.e. poor temperature dependence). So, the $Ca_{1.9}Eu_{0.1}Si_5N_8$ phosphor has a low quenching temperature, i.e. ~ 360 K. Compared with the large Stokes shift, a large centroid shift ε_c and the crystal field splitting ε_{cfs} are key factors to improve red phosphors for warm-white LEDs because they result in a large red-shift of the Eu^{2+} emission without worsening their thermal quenching. $Ca_{1.9}Eu_{0.1}Si_5N_8$ has an ex-

citation band centred at the ~ 2.51 eV, emission band centred at ~ 2.01 eV, and a thermal quenching above room temperature. Therefore, it can be a promising phosphor for warm white LEDs.

5. Conclusion

$Ca_2Si_5N_8$:Eu^{2+} phosphor for warm white light-emitting diodes is synthesized through a solid-state reaction. Rietveld refinement of the crystal structure of $Ca_{1.9}Eu_{0.1}Si_5N_8$ reveals that Eu atoms substituting for Ca atoms occupy two crystallographic positions. Broad emission and excitation bands observed are attributed to the transitions between the $^8S_{7/2}$ ground level of the $4f^7$ configuration and the crystal field components of the $4f^6 5d$ excited state. The emission band consists of two Gaussians, which correspond to two Eu^{2+} sites in the structure. The centroid shift ε_c and the crystal field splitting ε_{cfs} of the $5d$ levels of Eu^{2+} are evaluated to be 1.17 eV and 1.79 eV, respectively. The temperature dependence of PL is analysed by using a configuration coordinate model with the Huang–Rhys parameter $S = 6.0$ and the phonon energy $\hbar\nu = 52$ meV. The Stokes shift is calculated to be 0.57 eV. The emission intensity maximum occurring at ~ 200 K can be explained by the trapping effect. Strong decreases of both PL intensities and decay time with temperature increasing above 200 K are due to the non-radiative process dominating. The $Ca_{1.9}Eu_{0.1}Si_5N_8$ compound can be a promising phosphor for warm white LEDs because it has a sub-excitation band centred at ~ 2.51 eV and an emission band centred at ~ 2.01 eV.

References

[1] Malakoff D 2002 *Science* **296** 1782
[2] Nakamura S and Fasol G 1997 *The Blue Laser Diode: GaN Based Light Emitters and Lasers* (Berlin: Springer)
[3] Rajamohan Reddy K, Annapurna K and Buddhudu S 1996 *Mater. Lett.* **28** 489
[4] Xie R J, Hirosaki N, Sakuma K, Yamamoto Y and Mitomo M 2004 *Appl. Phys. Lett.* **84** 5404
[5] Li Y Q, van Steen J E J, van Krevel J W H, Botty G, Delsing A C A, DiSalvo F J, de With G and Hintzen H T J 2006 *Alloys Compd.* **417** 273
[6] Yamashita N, Harada O and Nakamura K 1995 *Jpn. J. Appl. Phys.* **34** 5539
[7] Jorgensen C K 1971 *Modern Aspects of Ligand Field Theory* (Amsterdam: Noth-Holland Publishing Company)
[8] Dorenbos P J 2003 *Lumin.* **104** 239
[9] Piao X Q, Machida K, Horikawa T and Hanzawa H J 2008 *Electrochem. Soc.* **155** J17
[10] Li Y Q, de With G and Hintzen H T J 2003 *Solid State Chem.* **181** 515
[11] Höppe H A, Lutz H, Morys P, Schnick W and Seilmeier A J 2000 *Phys. Chem. Solids.* **61** 2001
[12] Piao X Q, Horikawa T, Hanzawa H and Machida K J 2006 *Electrochem. Soc.* **153** H232
[13] Xie R J, Hirosaki N, Suehiro T, Xu F F and Mitomo M 2006 *Chem. Mater.* **18** 5578
[14] Schlieper T and Schnick W Z 1995 *Anorg. Allg. Chem.* **621** 1037
[15] Rietveld H M 1967 *Acta Crystallogr.* **229** 151
[16] Rietveld H M 1969 *J. Appl. Crystallogr.* **2** 65
[17] Hill R J and Howard C J J 1987 *Appl. Cryst.* **20** 467
[18] Aull B F and Jenssen H P 1986 *Phys. Rev.* B **34** 6640
[19] Chartier C, Barthou C, Benalloul P and Frigerio J M J 2005 *Lumin.* **111** 147
[20] Henderson B and Imbusch G F 1989 *Optical Spectroscopy of Inorganic Solids* (Oxford: Clarendon Press)
[21] Dorenbos P 2000 *Phys. Rev.* B **62** 15640